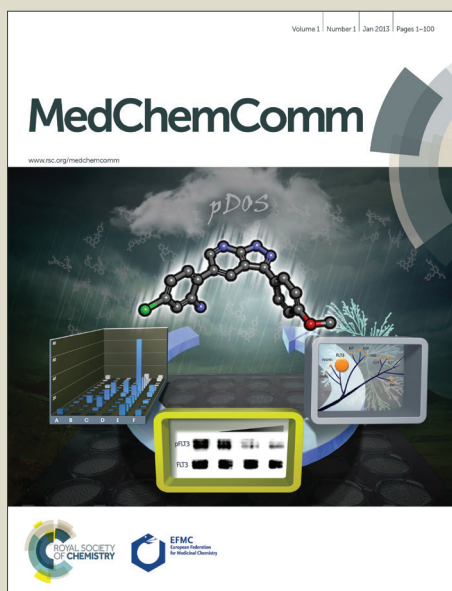


# MedChemComm

Accepted Manuscript



This is an *Accepted Manuscript*, which has been through the Royal Society of Chemistry peer review process and has been accepted for publication.

*Accepted Manuscripts* are published online shortly after acceptance, before technical editing, formatting and proof reading. Using this free service, authors can make their results available to the community, in citable form, before we publish the edited article. We will replace this *Accepted Manuscript* with the edited and formatted *Advance Article* as soon as it is available.

You can find more information about *Accepted Manuscripts* in the [Information for Authors](#).

Please note that technical editing may introduce minor changes to the text and/or graphics, which may alter content. The journal's standard [Terms & Conditions](#) and the [Ethical guidelines](#) still apply. In no event shall the Royal Society of Chemistry be held responsible for any errors or omissions in this *Accepted Manuscript* or any consequences arising from the use of any information it contains.



Journal Name

ARTICLE

## Discovery, synthesis and structure-activity analysis of symmetrical 2,7-disubstituted fluorenones as urea transporter inhibitors

Sujin Lee<sup>a</sup>, Cristina Esteva-Font<sup>a</sup>, Puay-Wah Phuan<sup>a</sup>, Marc O. Anderson<sup>b</sup>, and A.S Verkman<sup>a</sup>

Received 00th January 20xx,  
Accepted 00th January 20xx

DOI: 10.1039/x0xx00000x

www.rsc.org/

Kidney urea transporters are targets for development of small-molecule inhibitors with action as salt-sparing diuretics. A cell-based, functional high-throughput screen identified 2,7-bisacetamido fluorenone **3** as a novel inhibitor of urea transporters UT-A1 and UT-B. Here, we synthesized twenty-two 2,7-disubstituted fluorenone analogs by acylation. Structure-activity relationship analysis revealed: (a) the carbonyl moiety at C9 is required for UT inhibition; (b) steric limitation on C2, 7-substituents; and (c) the importance of a crescent-shape structure. The most potent fluorenones inhibited UT-A1 and UT-B urea transport with  $IC_{50} \sim 1 \mu M$ . Analysis of in vitro metabolic stability in hepatic microsomes indicated metabolism of 2,7-disubstituted fluorenones by reductase and subsequent elimination. Computational docking to a homology model of UT-A1 suggested UT inhibitor binding to the UT cytoplasmic domain at a site that does not overlap with the putative urea binding site.

The kidney expresses urea transporter (UT) proteins, which facilitate the passive transport of urea across cell plasma membranes in a subset of kidney tubules and microvessels.<sup>1</sup> SLC14A1 and SLC14A2 genes encode UT-A and UT-B urea transporters, respectively.<sup>2</sup> Studies in mice lacking UTs<sup>3-7</sup> and in rodents treated with UT inhibitors<sup>8-10</sup> indicate that UT-A1, the UT-A isoform expressed at the apical membrane of epithelial cells in inner medullary collecting duct, is the principal target for diuretic development. Absence or inhibition of UTs impairs urinary concentrating function, producing a diuretic response. UT inhibitors are thus development candidates as first-in-class salt-sparing diuretics for therapy of various edema states and hyponatremias, such as those associated with congestive heart failure and cirrhosis.<sup>11-13</sup>

Our lab previously developed high-throughput functional assays of UT-A<sup>14</sup> and UT-B<sup>15</sup> urea transporters. Several classes of small-molecule inhibitors of the target UT-A1 were identified.<sup>10, 14</sup> In proof-of-concept studies, two classes of inhibitors with low micromolar  $IC_{50}$  produced a diuretic response in rats;<sup>10</sup> however, their inhibition potency and metabolic stability were not optimal for further development. Additional screening reported here identified symmetrical, disubstituted fluorenones as novel UT inhibitors. Because of the drug-like properties of tricyclic fluorenones and the absence of a commercial source to obtain analogs for structure-activity

relationship analysis, here we synthesized 22 symmetrical, disubstituted fluorenones, measured their UT inhibition activity and selectivity, analyzed their inhibition and metabolism mechanisms, and used homology modeling and computational docking to propose binding sites on UT-A and UT-B.

A UT-A1 inhibition screen of 50,000 compounds identified 2,7-bisacetamidofluorenone **3** as a UT-A1 inhibitor with  $IC_{50} \sim 1 \mu M$  that produced complete inhibition at higher concentrations (**Fig. 1A**). Fluorenone **3** also inhibited UT-B with similar potency. The fluorenone scaffold has not been previously reported for the inhibition of urea transporters, though there are prior reports of biological activities of this compound class. Tilonon is an orally bioavailable antiviral agent<sup>16, 17</sup> and an immunomodulator.<sup>18</sup> The antitumor activity of fluorenone derivatives has been shown to be result from inhibition of telomerase and DNA topoisomerase I.<sup>19-21</sup> Most reported fluorenone analogs focused on 2,7-bis-ester or ether moieties, unlike the bis-acetamidofluorenone **3** identified from the UT-A1 screen. The 2,7-bis-acetamido fluorenone structure has drug-like properties, including favorable molecular weight (294 Da), topological surface area (75.2 Å<sup>2</sup>) and cLogP (2.12), which fall within the Lipinski<sup>22</sup> and Veber<sup>23</sup> criteria for orally bioavailable drugs.

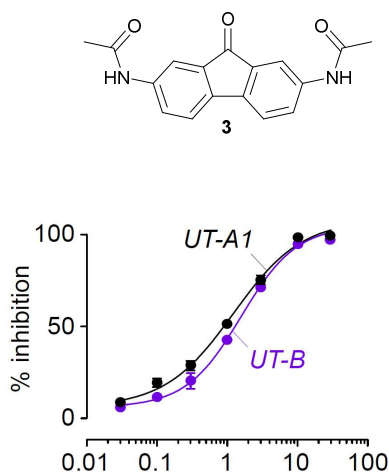
Based on the potency and physicochemical properties of **3**, a series of 2,7-disubstituted fluorenone analogs were rationally designed to identify more potent urea transport inhibitors and to establish structure-activity relationships. Structurally, fluorenone **3** is a symmetrical, rigid crescent-shaped molecule with a carbonyl group at the 9-position and bisacetamido groups at the 2 and 7 positions.

<sup>a</sup> Departments of Medicine and Physiology, University of California, San Francisco CA, 94143-0521 USA.

<sup>b</sup> Department of Chemistry and Biochemistry, San Francisco State University, San Francisco CA, 94132-4136 USA.

† Electronic Supplementary Information (ESI) available: [details of any supplementary information available should be included here]. See DOI: 10.1039/x0xx00000x

A



B

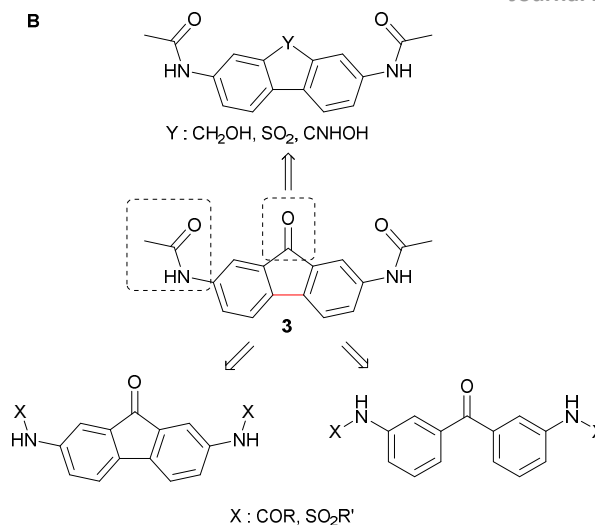
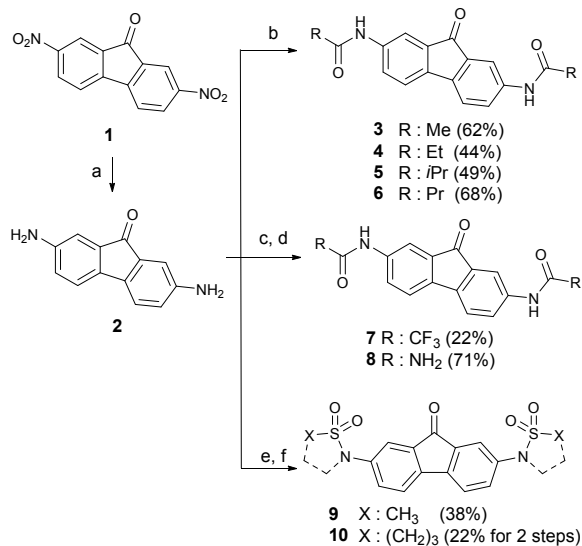


Fig 1. Discovery of 2,7-disubstituted fluorenone **3** as UT-A1 inhibitor. A. Structure of **3** and concentration-inhibition data for inhibition of rat UT-A1 and UT-B urea transporters. Fitted parameters: IC<sub>50</sub> 1 μM and 1.5 μM, Hill coefficient 0.9 and 1.1, for UT-A1 and UT-B respectively. B. Strategy for analogs synthesis for SAR analysis.

As diagrammed in **Fig. 1B**, analogs were designed to include: i) different functional groups on the 2,7-diamino position; ii) different non-carbonyl functional groups at the 9-position; and iii) flexible and ring strain-released scaffolds. In a preliminary study, testing of ~70 commercially available fluorenone analogs did not identify active analogs.

**Scheme 1** shows the synthetic approaches for the preparation of 2,7-bis(alkylamido)fluorenone **3-10**. Reduction of commercially available 2,7-dinitro-fluorenone-9-one **1** using sodium sulfide nonahydrate and sodium hydroxide afforded the key intermediate 2,7-diamino-fluorenone-9-one **2**.<sup>19</sup> The re-synthesis of **3** was accomplished by acetylation of **2** using

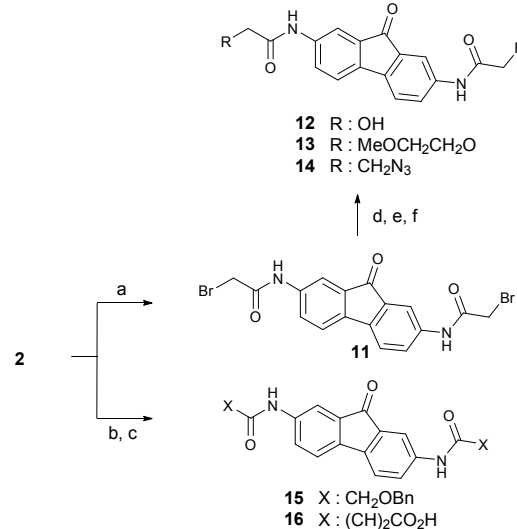


Scheme 1. Synthesis of 2,7-bis(alkylamido)fluorenone and 2,7-bisulfonamidofluorenone analogs.

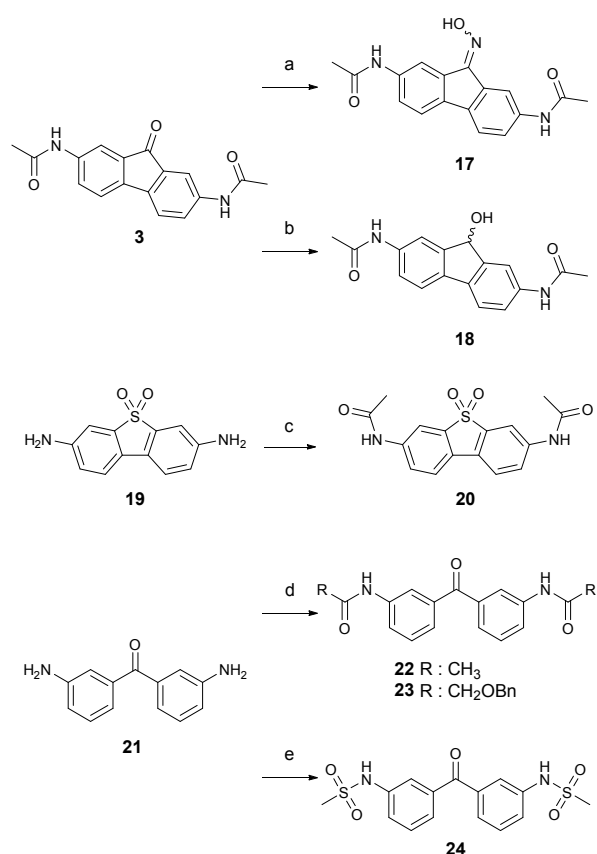
Reaction conditions and reagents: (a) Na<sub>2</sub>S·9H<sub>2</sub>O, NaOH, EtOH, 78%; (b) Et<sub>3</sub>N, THF, Ac<sub>2</sub>O for **3**, propionyl chloride for **4**; isobutryl chloride for **5**; butyryl chloride for **6**; (c) CF<sub>3</sub>CO<sub>2</sub>H in a sealed tube for **7**; (d) KNCO, AcOH/H<sub>2</sub>O for **8**; (e) MsCl, pyridine, THF for **9**; (f) 3-chloropropanesulfonyl chloride, pyridine, CH<sub>2</sub>Cl<sub>2</sub>; then, K<sub>2</sub>CO<sub>3</sub>, CH<sub>3</sub>CN, reflux, for **10**.

acetic anhydride. Additional acyl analogs of **3** were similarly prepared by reaction of **2** with the respective acyl reagents under basic condition to yield propionyl, isobutyryl and butyryl analogs **4**, **5** and **6** respectively. We next prepared the bioisostere analogs of **3**, trifluoroacetamide **7**, carbamate **8** and methanesulfonamide **9**. Treatment of **2** with trifluoroacetic acid and heating to reflux in a sealed tube afforded trifluoroacetamide **7**.<sup>24</sup> The carbamate analog **8** was synthesized by reaction of **2** with potassium isocyanate.<sup>25</sup> Sulfonamide analog **9** was prepared by mesylation in pyridine. The  $\gamma$ -sultam **10** was synthesized using chloropropanesulfonyl chloride and subsequent cyclization with potassium carbonate.

As shown in **Scheme 2**, analogs with extended chains on the amide bond were synthesized. Bromoacetamido **11** and



Scheme 2. Synthesis of extended 2,7-bis(alkylamido)fluorenone analogs. Reaction conditions and reagents: (a) bromoacetyl bromide, xylene, reflux, 40%; (b) benzyloxyacetyl chloride, xylene, reflux, 26% for **15**; (c) maleic anhydride, CHCl<sub>3</sub>, 26% for **16**; (d) NaOH, EtOH, 86% for **12**; (e) methoxyethanol, NaH, CH<sub>3</sub>CN, 18% for **13**; (f) NaN<sub>3</sub>, DMF, 24% for **14**.



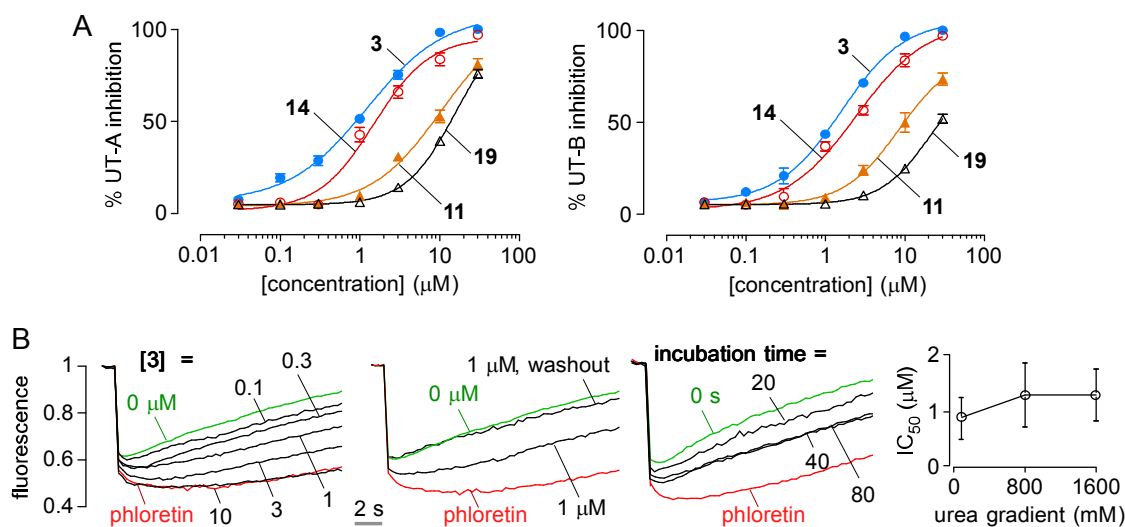
Scheme 3. Synthesis of carbonyl-modified fluorenone analogs. Reaction conditions and reagents: (a)  $\text{NH}_2\text{OH}\cdot\text{HCl}$ ,  $\text{DMSO}/\text{H}_2\text{O}$ , 22%; (b)  $\text{NaBH}_4$ ,  $\text{CH}_3\text{CN}/\text{MeOH}$  (10/1), 28%; (c)  $\text{Et}_3\text{N}$ ,  $\text{THF}$ ,  $\text{Ac}_2\text{O}$ , 65%; (d)  $\text{Et}_3\text{N}$ ,  $\text{THF}$ ,  $\text{Ac}_2\text{O}$ , 62% for **22**; Benzoyloxyacetyl chloride, xylene, reflux, 46% for **23**; (e)  $\text{MsCl}$ , pyridine,  $\text{THF}$ , 23%.

benzyloxyacetamido **15** were synthesized from **2** using corresponding acyl halides in refluxing xylene. Using maleic

anhydride in refluxing chloroform gave the maleamic acid analog **16**. Further substitution reaction of **11** using methoxyethanol with sodium hydride afforded **13**, and with sodium hydroxide and sodium azide gave the corresponding amide analogs **12** and **14**, respectively.

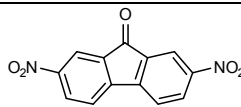
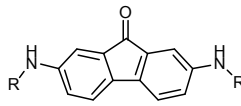
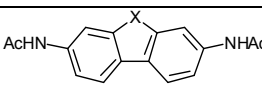
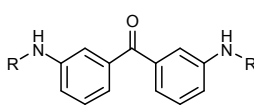
To investigate the importance of the carbonyl at the 9-position for urea transport inhibition, we synthesized oxime **17**, hydroxyl **18** and sulfone **20** (Scheme 3). Condensation of 2,7-bisacetamido fluorenone-9-one **3** with hydroxylamine hydrochloride in pyridine afforded oxime analog **17**. Ketone reduction of **3** with sodium borohydride in methanol gave hydroxyl analog **18**. Acylation of commercially available 2,7-diaminodiphenylsulfone **19** afforded the bisacetamidodiphenylsulfone **20**. To prepare flexible ring acyclic analogs, commercially available 3,3'-diaminobenzophenone **21** was acylated and sulfonated to give bisacetamide **22**, benzyloxyacetamide **23** and bismethanesulfonamidobenzophenone **24**.

**Table 1** summarizes  $\text{IC}_{50}$  values for inhibition of UT-A1 and UT-B urea transport by the 2,7-disubstituted fluorenone **1-24**. Most analogs showed similar  $\text{IC}_{50}$  for inhibition of UT-A1 and UT-B urea transport. Non-substituted fluorenone (**1**, **2** and **21**) were inactive. Elongation of the carbon chain on the amide reduced inhibition, comparing acetamide **3** to propionyl **4**, isobutyryl **5**, maleamic acid **16** and butyryl **6**. Linear ether linkage analogs with elongated side chain also reduced inhibition. Hydroxyacetamide **12** had low activity, and benzyloxyacetamides **15** and **13** were inactive. Replacing acetamide with methanesulfonylamide **9** and carbamate **8** slightly reduced activity. Addition to the acetamide of one more atom - hydroxyl **12**, methyl **4** or bromide **11** - reduced activity. These findings implicate a narrow size limitation for substituents. Interestingly, trifluoroacetamide **7**, which has the same carbon length as **3**, was much less active, indicating that steric and electronic effects also influence inhibition.



**Fig. 2.** Urea transport inhibition by 2,7-disubstituted fluorenone. A. Concentration-inhibition data for UT-A1 and UT-B for **3**, **11**, **14** and **19**. B. Primary data from UT-A inhibition assay showing reversibility, inhibition kinetics and urea competition for **3**. Phloretin concentration was 0.35 mM.

**Table 1.** Inhibition of UT-A1 and UT-B urea transport by 2,7-disubstituted fluorenone analogs.

Structure	Functional group	UT-A1 IC <sub>50</sub> (μM)	UT-B IC <sub>50</sub> (μM)
	<b>1</b>	>50	>50
	<b>R</b>		
	<b>2</b> H	>50	>50
	<b>3</b> COCH <sub>3</sub>	1	1.5
	<b>4</b> COCH <sub>2</sub> CH <sub>3</sub>	15	5
	<b>5</b> COCH(CH <sub>3</sub> ) <sub>2</sub>	18	50
	<b>6</b> CO(CH <sub>2</sub> ) <sub>2</sub> CH <sub>3</sub>	>50	>50
	<b>7</b> COCF <sub>3</sub>	10	7.5
	<b>8</b> CONH <sub>2</sub>	2	1.2
	<b>9</b> SO <sub>2</sub> CH <sub>3</sub>	1.5	2.5
	<b>10</b> SO <sub>2</sub> (CH <sub>2</sub> ) <sub>3</sub>	>50	>50
	<b>11</b> COCH <sub>2</sub> Br	30	10
	<b>12</b> COCH <sub>2</sub> OH	20	25
	<b>13</b> COCH <sub>2</sub> O(CH <sub>2</sub> ) <sub>2</sub> OMe	>50	50
	<b>14</b> COCH <sub>2</sub> N <sub>3</sub>	20	30
	<b>15</b> COCH <sub>2</sub> OBn	>50	>50
	<b>16</b> CO(CH <sub>2</sub> ) <sub>2</sub> CO <sub>2</sub> H	30	>50
	<b>X</b>		
	<b>17</b> CNHOH	12	25
	<b>18</b> CHOH	>50	20
	<b>20</b> SO <sub>2</sub>	15	2
	<b>R</b>		
	<b>21</b> H	>50	>50
	<b>22</b> COCH <sub>3</sub>	18	20
	<b>23</b> COCH <sub>2</sub> OBn	>50	>50
	<b>24</b> SO <sub>2</sub> CH <sub>3</sub>	>50	30

The influence of the carbonyl moiety was determined by comparing UT-A1 inhibition by **3**, **17**, **18** and **20**. These analogs contain acetamide on the C2 and C7 positions, but activity was reduced greatly by replacing the carbonyl with oxime **17**, sulfone **20** or hydroxyl **18** moieties (IC<sub>50</sub> 12 to >50 μM), suggesting that a hydrogen bond acceptor is necessary on the carbonyl. Interestingly, sulfone **20** showed UT-B selectivity with IC<sub>50</sub> of 2 μM for UT-B compared to 15 μM for UT-A1.

**Fig. 2A** shows concentration-inhibition data for UT-A1 and UT-B inhibition by **3** and analogs **7**, **9** and **22**. **Fig. 2B** shows original concentration-inhibition curves for **3** (left panel). The *in vitro* characterization of **3** revealed complete reversibility for inhibition of UT-A1 (second panel), rapid inhibition kinetics with complete inhibition by 40 seconds (third panel), and a non-competitive inhibition mechanism in which apparent IC<sub>50</sub> was independent of urea concentration (right panel).

To investigate the potential utility of disubstituted fluorenone for UT inhibition in animal studies, *in vitro* microsomal stability measurements were made using an established assay in which compounds were incubated with rat liver microsomes in the presence of NADPH.<sup>26</sup> For **3**, 60% remained after 15 min (**Fig. 3A**). Oxidation catalyzed by the cytochrome P450

monooxygenase, a well-known metabolic reaction on aromatic compounds, was not detected from LC/MS analysis. Instead, a peak at [M+H-16] was detected that increased over time (**Fig. 3B**). Generation of a [M+H-16] metabolite suggests loss of oxygen, suggesting that bisacetamidofluorenone metabolism involves the mechanism proposed in **Fig. 4**. Carbonyl reduction of 2,7-dinitrofluorenone by rat liver enzymes utilizing NADH/NADPH has been reported, although the specific carbonyl reduction enzyme was not established.<sup>27</sup> Following reduction of carbonyl on fluorenone, the amide proton is readily removed by base-catalyzed elimination to give 2-iminofluorene **25**. To support this proposed mechanism, fluorenone **18** was subjected to basic condition (1M NaOH). The eliminated product **25** could be isolated after 1 hour in ~60% yield, and matched [M+H-16].<sup>28</sup> Also, to confirm this proposed mechanism, metabolic stability was studied for oxime **17**,

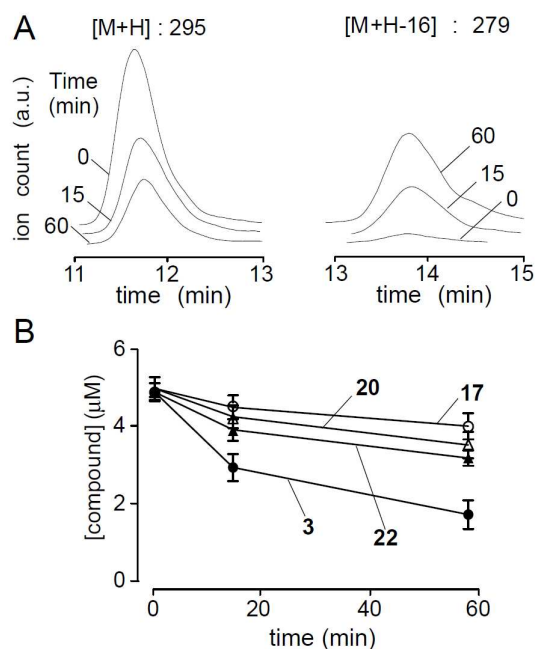


**Fig. 3.** *In vitro* metabolic stability of disubstituted fluorenone. Compounds incubated with hepatic microsomes in the presence of NADPH. **A.** LC/MS showing disappearance of **3** and appearance of metabolite over 60 min. **B.** Kinetics of disappearance of **3**, **17**, **20**, and **22** over 60 min.

bisacetaminobiphenylacetone **22** and bisacetaminosulfone **20**, which do not contain a carbonyl moiety and thus cannot undergo carbonyl reduction/base-catalyzed elimination sequence. We found that **17**, **20** and **22** were relatively stable compared to fluorenone **3** (>80% remaining at 15 min), and [M+H-16] was not detected by LC/MS (data not shown).

Interestingly, acetophenone analog **22** had less UT inhibition activity than **3** and sulfonamide **24** was inactive compared to corresponding fluorenone analog **9**, which showed strong inhibition. This result suggests that the 3D structure of the fluorenone core is important to UT inhibition. Fluorenone with 2,7-disubstituents have a crescent-like shape, which is lost when substituted with biphenylacetone. Increasing flexibility of the acetophenone moiety reduced UT inhibition activity.



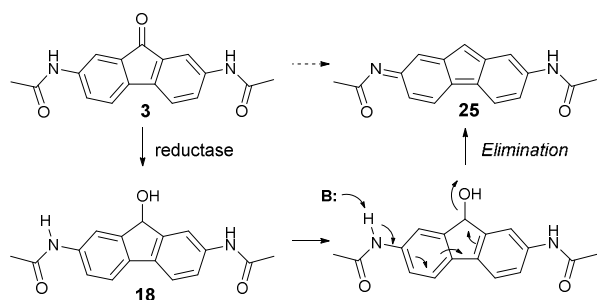


Fig. 4. Proposed mechanism of hepatic metabolism of **3**.

Computational docking simulations were done to propose binding modes for the most potent UT-A1 inhibitor **3**, and the most potent UT-B inhibitor **8**. Structures for rat UT-A1 and UT-B were generated by homology modeling as described,<sup>10</sup> based on the high resolution X-ray crystal structure of bovine UT-B solved at 2.5Å.<sup>29</sup> Our homology models of these two proteins contain sites that appear homologous to narrow constriction (Sm) and low energy urea binding sites (So and Si) observed in the bovine UT-B template structure.

**Fig. 5A** shows docked conformations of inhibitor **3** bound to UT-A1 and UT-B. The lowest energy conformation of this molecule docked into both proteins in similar orientations. The planar inhibitor scaffold docked into the outer part of the UT-A1 and UT-B pore region, not binding deeply into the channel. In the docked conformation of **3** with UT-A1 the amido NH<sub>2</sub> group projects into a pocket surrounded by Glu<sup>572</sup>, Val<sup>603</sup>, Asn<sup>604</sup>, Phe<sup>832</sup> and Tyr<sup>900</sup>. The bis-urea inhibitor **8**, which shows a greater potency for UT-B, is shown for comparison (**Fig. 5B**), and docks in a similar manner as **3**. Other active analogs of **3** also docked similarly. The position of the inhibitor

scaffolds do not overlap the putative cytoplasmic urea binding site (Si) near Gln<sup>599</sup>, which is homologous to Gln<sup>63</sup> in the selenourea-bound template structure.<sup>28</sup> Taken together with urea competition experiments for **3**, the proposed binding site in **Fig. 5** is consistent with a non-competitive inhibition mechanism.

## Conclusions

In conclusion, we identified by high-throughput screening symmetrical 2,7-disubstituted fluorenones as novel UT inhibitors, and established structure-activity relationships by synthesis and characterization of 22 analogs. Functional studies indicated reversible inhibition of UT-A1 urea transport by the 2,7-disubstituted fluorenone analogs by a non-competitive inhibition mechanism. Docking computations suggested inhibitor binding at the UT outer pore regions at a site distinct from the putative urea binding site. Finally, analysis of inhibitor metabolism indicated carbonyl reduction by reductase and subsequent base-catalyzed elimination.

## Experimentals

**Synthesis.** All chemical synthetic procedures and characterizations are described in supplementary information.

**Cell culture.** Triply transfected MDCK cells expressing rat UT-A1, yellow fluorescent protein (YFP)-H148Q/V163S and human aquaporin-1 (AQP1) were grown in Dulbecco's modified Eagle medium, 10% FBS and three selection antibiotics (zeocin, geneticin and hygromycin B), as described.<sup>14</sup>

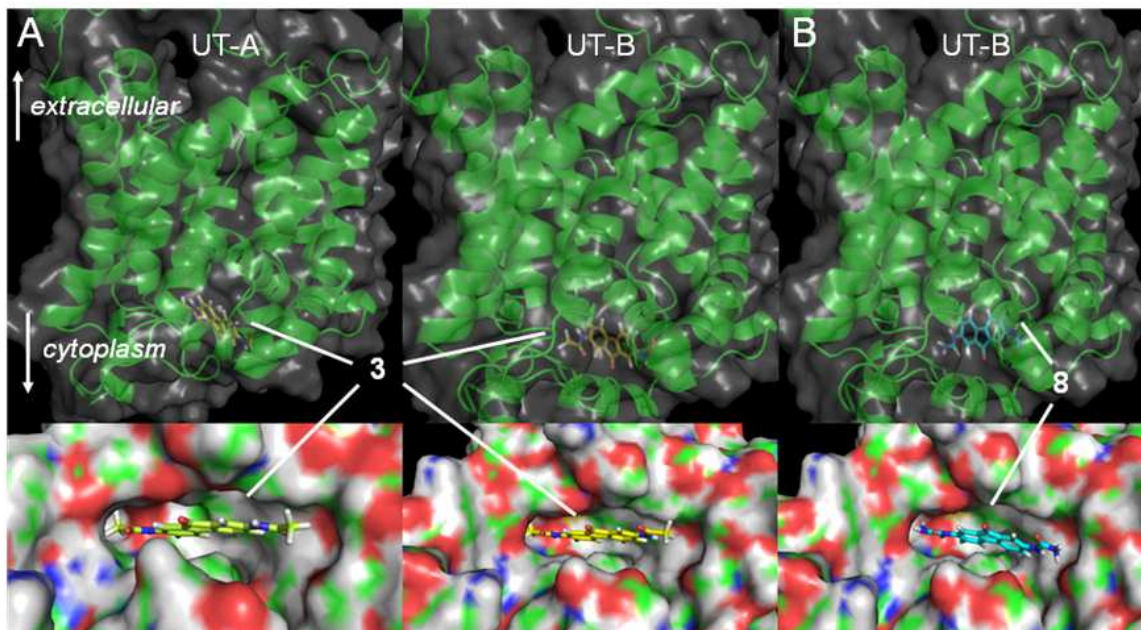


Fig. 5. Computational docking of **3** and **8** to homology models of rat UT-A and UT-B. Zoomed-in and zoomed-out representations of (A) inhibitor **3** bound to rat UT-A and UT-B cytoplasmic domains; and (B) the most potent UT-B inhibitor **8** bound to the rat UT-B cytoplasmic domain.

**UT-A1 inhibition assay.** MDCK-UT-A1-AQP1-YFP cells were used for UT-A1 inhibition assay as described.<sup>14</sup> Briefly, after incubation for 15 min with compounds the cells were subjected to a 800 mM urea gradient and cellular YFP fluorescence was continuously measured with a plate reader (model Infinite M1000, Tecan Trading AG, Switzerland). UT-A1 inhibition alters the profile of the curve, increasing the initial shrinkage (decreased fluorescence) and slowing reswelling (increased fluorescence). Percentage UT-A1 inhibition was computed as  $100\% (F_{\text{neg}} - F_{\text{test}})/(F_{\text{neg}} - F_{\text{pos}})$ , where F is fluorescence measured 7 s after urea injection for the negative control ( $F_{\text{neg}}$ ), test compound ( $F_{\text{test}}$ ) and positive control ( $F_{\text{pos}}$ ).

**UT-B inhibition assay.** As described,<sup>15</sup> whole rat blood was diluted to a hematocrit of ~1.5% in PBS containing 1.25 M acetamide. Erythrocyte suspensions were incubated for 15 min with test compounds and then rapidly mixed with PBS. Percentage lysis was quantified from absorbance at 710 nm as:  $100\% (A_{\text{neg}} - A_{\text{test}})/(A_{\text{neg}} - A_{\text{pos}})$ , where A is absorbance for the negative control ( $A_{\text{neg}}$ ), test compound ( $A_{\text{test}}$ ) and positive control ( $A_{\text{pos}}$ ) at 710 nm.

**Functional studies.** Reversibility was tested by incubation of inhibitors at a concentration near their  $IC_{50}$  and then washing with PBS before UT-A1 inhibition assay. Competition with urea was studied using different concentrations of urea (80 to 1,600 mM) in the UT-A1 inhibition assay.

## Acknowledgements

Supported by grants DK101373, DK35124, DK72517, EB00415 and EY13574 from the National Institutes of Health. The authors acknowledge OpenEye Scientific (Santa Fe, NM, USA) for its Academic Site License program.

## Notes and references

- Klein, J. D., Blount, M. A., Sands, J. M., Urea transport in the kidney, *Compr. Physiol.* **2011**, *2*, 699–729.
- Smith, C. P., Mammalian urea transporters, *Exp Physiol.* **2009**, *94*, 180–185.
- Fenton, R. A., Chou, C. L., Stewart, G. S., Smith, C. P., Knepper, M. A., Urinary concentrating defect in mice with selective deletion of phloretin-sensitive urea transporters in the renal collecting duct, *Proc. Natl. Acad. Sci.* **2004**, *101*, 7469–7474.
- Fenton, R. A., Flynn, A., Shodeinde, A., Smith, C. P., Schnermann, J., Knepper, M. A., Renal phenotype of UT-A urea transporter knockout mice, *J. Am. Soc. Nephrol.* **2005**, *16*, 1583–1592.
- Uchida, S., Sohara, E., Rai, T., Ikawa, M., Okabe, M., Sasaki, S., Impaired urea accumulation in the inner medulla of mice lacking the urea transporter UT-A2, *Mol. Cell Biol.* **2005**, *25*, 7357–7363.
- Klein, J. D., Frohlich, O., Mistry, A. C., Kent, K. J., Martin, C. F., Sands, J. M., Transgenic mice expressing UT-A1, but lacking UT-A3, have intact urine concentration ability, *FASEB. J.* **2013**, *27*, 1111–1117.
- Yang, B., Bankir, L., Gillespie, A., Epstein, C. J., Verkman, A. S., Urea-selective concentrating defect in transgenic mice lacking urea transporter UT-B, *J. Biol. Chem.*, **2002**, *277*, 10633–10637.
- Yao, C., Anderson, M. O., Zhang, J., Yang, B., Phuan, P. W., Verkman, A. S., Triazolothieno-pyrimidine inhibitors of urea transporter UT-B reduce urine concentration, *J. Am. Soc. Nephrol.*, **2012**, *23*, 1210–1220.
- Li, F., Lei, T., Zhu, J., Wang, W., Sun, Y., Chen, J., Dong, Z., Zhou, H., Yang, B., A novel small-molecule thienoquinolin urea transporter inhibitor acts as a potential diuretic, *Kidney Int.*, **2013**, *83*, 1076–1086.
- Esteva-Font, C., Cil, O., Phuan, P. W., Su, T., Lee, S., Anderson, M. O., Verkman, A. S., Diuresis and reduced urinary osmolality in rats produced by small-molecule UT-A-selective urea transport inhibitors, *FASEB. J.*, **2014**, *28*, 3878–3890.
- Knepper, M. A. and Miranda, C. A., Urea channel inhibitors: a new functional class of aquaretics, *Kidney Int.*, **2013**, *83*, 991–993.
- Sands, J. M., Renal urea transporters, *Curr. Opin. Nephrol. Hypertens.*, **2004**, *13*, 525–532.
- Esteva-Font, C., Anderson, M. O., Verkman, A. S., Urea transport proteins as drug targets, *Nat. Rev. Nephrol.*, **2015**, *11*, 113–123.
- Esteva-Font, C., Phuan, P. W., Anderson, M. O., Verkman, A. S., A small molecule screen identifies selective inhibitors of urea transporter UT-A, *Chem. Biol.*, **2013**, *20*, 1235–1244.
- Levin, M. H., De la Fuente, R., Verkman, A. S., Urearetics: a small molecule screen yields nanomolar potency inhibitors of urea transporter UT-B, *FASEB. J.*, **2007**, *21*, 551–563.
- Mayer, G.D. and Krueger, R. F., Tilorone hydrochloride: mode of action, *Science* **1970**, *169*, 1214–1215.
- Krueger, R. F. and Mayer, G. D., Tilorone hydrochloride: an orally active antiviral agent, *Science* **1970**, *169*, 1213–1214.
- Svensson, C. K., Knowlton, P. W., Effect of the immunomodulator tilorone on the in vivo acetylation of procainamide in the rat, *Pharm. Res.*, **1989**, *6*, 477–480.
- Perry, P. J., Read, M. A., Davies, R. T., Gowlan, S. M., Reszka, A. P., Wood, A. A., Kelland, L. R., Neidle, S., 2,7-Disubstituted Amidofluorenone Derivatives as Inhibitors of Human Telomerase, *J. Med. Chem.*, **1999**, *42*, 2679–2684.
- Lee, C.-C., Chang, D.-M., Huang, K.-F., Chen, C.-L., Chen, T.-C., Lo, Y., Guh, J.-H., Huang, H.-S., Design, synthesis and antiproliferative evaluation of fluorenone analogs with DNA topoisomerase I inhibitory properties, *Bioorg. Med. Chem.*, **2013**, *21*, 7125–7133.
- Zhou, D., Tuo, W., Hu, H., Xu, J., Chen, H., Rao, Z., Xiao, Y., Hua, X., Liu, P., Synthesis and activity evaluation of tilorone analogs as potential anticancer agents, *Eur. J. Med. Chem.*, **2013**, *64*, 432–441.
- Lipinski, C. A., Lombardo, F., Dominy, B. W., Feeney, P. J., Experimental and computational approaches to estimate solubility and permeability in drug discovery and development settings, *Adv. Drug. Deliv. Rev.*, **2001**, *46*, 3–26.
- Veber, D. F., Johnson, S. R., Cheng, H.-Y., Smith, B. R., Ward, K. W., Kopple, K. D., Molecular properties that influence the oral bioavailability of drug Candidates, *J. Med. Chem.* **2002**, *45*, 2615–2623.
- Fletcher, T. L., Taylor, M. E., Dahl, A. W., Derivatives of fluorine. I. N-Substituted 2-aminofluorene and 2-aminofluorenone, *J. Org. Chem.*, **1955**, *20*, 1021–1025.
- Perry, C. J., Holding, K., Tyrrell, E., Simple, novel synthesis for 1-carbamoyl-1H-benzotriazole and some of its analogs, *Syn. Commun.*, **2008**, *38*, 3354–3365.
- Snyder, D. S., Tradtrantip, L., Yao, C., Kurth, M. J., Verkman, A. S., Potent, metabolically stable benzopyrimidopyrrolo-oxazine-dione (BPO) CFTR inhibitors for polycystic kidney disease, *J. Med. Chem.*, **2011**, *54*, 5468–5477.
- Ritter, C. L., Decker, R. W., Malejka-Giganti, D., Reduction of nitro and 9-oxo groups of environmental nitrofluorenes by the rat mammary gland in vitro, *Chem. Res. Toxicol.*, **2000**, *13*, 793–800.

- 28 Compound **25**:  $^1\text{H}$  NMR ( $\text{DMSO-}d_6$ )  $\delta$  10.13 (brs, 1H), 7.78 (brs, 1H), 7.57 (d, 1H,  $J = 8.0$  Hz), 7.37 (d, 1H,  $J = 7.8$  Hz), 7.28 (d, 1H,  $J = 8.0$  Hz), 6.79 (brs, 1H), 6.66 (d, 1H,  $J = 8.1$  Hz), 5.57 (brs, 1H), 2.55 (s, 3H), 2.05 (s, 3H); LRMS (ESI)  $m/z$  279 ( $\text{M}+\text{H}$ ) $^+$ .
- 29 Levin, E. J., Cao, Y., Enkavi, G., Quick, M., Pan, Y., Tajkhorshid, E., and Zhou, M. Structure and permeation mechanism of a mammalian urea transporter. *Proc. Natl. Acad. Sci.*, **2012**, *109*, 11194–11199.